arXiv:1708.05764v1 [math.NA] 18 Aug 2017

# APPROXIMATION BY HERGLOTZ WAVE FUNCTIONS*

FERNANDO GUEVARA VASQUEZ† AND CHINA MAUCK†

**Abstract.** We consider the problem of approximating a function using Herglotz wave functions, which are a superposition of plane waves. When the discrepancy is measured in a ball, we show that the problem can essentially be solved by considering the function we wish to approximate as a source distribution and time reversing the resulting field. Unfortunately this gives generally poor approximations. Intuitively, this is because Herglotz wave functions are determined by a two-dimensional field and the function to approximate is three-dimensional. If the discrepancy is measured on a plane, we show that the best approximation corresponds to a low-pass filter, where only the spatial frequencies with length less than the wavenumber are kept. The corresponding Herglotz wave density can be found explicitly. Our results have application to designing standing acoustic waves for self-assembly of micro-particles in a fluid.

**Key words.** Herglotz wave function, wave control, acoustic radiation force, time reversal

**AMS subject classifications.** 35J05,74J05,41A29

## 1. Introduction.

We study the problem of finding the best approximation of a function by *Herglotz wave functions*, which are functions of the form

$$u(\vec{\boldsymbol{x}}) = \int_{S(0,k)} g(\vec{\boldsymbol{x}}) \exp[i\vec{\boldsymbol{x}} \cdot \vec{\boldsymbol{z}}] dS(\vec{\boldsymbol{z}}), \tag{1}$$

where the integral is over the sphere $S(0,k) \equiv \{\vec{\boldsymbol{x}} \in \mathbb{R}^3 \mid |\vec{\boldsymbol{x}}| = k\}$, $k = 2\pi/\lambda$ is the wavenumber corresponding to a wavelength $\lambda$ and we refer to $g(\vec{\boldsymbol{x}})$ as a *Herglotz wave density*[1]. Herglotz wave functions are entire solutions to the Helmholtz equation $\Delta u + k^2 u = 0$.

The application we have in mind for this approximation problem is ultrasound directed self-assembly of micro-particles [7, 8, 14], where micro-particles in a fluid are controlled with standing acoustic waves. For this application, the fluid pressure $u$ inside a reservoir $D$ (an open subset of $\mathbb{R}^3$) with Lipschitz boundary $\partial D$ satisfies

$$\begin{aligned} \Delta u + k^2 u = 0 \text{ in } D, \text{ and} \\ \vec{\boldsymbol{n}} \cdot \nabla u + ik\alpha u = \phi \text{ on } \partial D, \end{aligned} \tag{2}$$

where $\vec{\boldsymbol{n}}(\vec{\boldsymbol{x}})$ is the unit outward pointing normal vector to the boundary and $\alpha(\vec{\boldsymbol{x}})$ is a function representing the boundary impedance of $\partial D$. The reservoir boundary $\partial D$ is assumed to be lined with transducers and the external excitation $\phi(\vec{\boldsymbol{x}})$ models the transducer operating parameters, i.e. the amplitude and phase of the voltage driving the transducers. The problem is to find transducer operating parameters $\phi$ such that particles cluster in a desired pattern, e.g. a surface or a curve. If the particles are neutrally buoyant in the fluid and less compressible than the fluid, the particles are known to cluster about the nodal or zero level set of the pressure, i.e. $\{\vec{\boldsymbol{x}} \in D \mid u(\vec{\boldsymbol{x}}) = 0\}$ (see e.g. [15]). The strategy we propose is to construct a function $f$ defined on $D$, with nodal set containing the desired pattern. If $v$ is a Herglotz wave function that is close enough to $f$, we expect their nodal sets to be close as well. Thus

* **Funding:** Army Research Office Contract No. W911NF-16-1-0457.

†Mathematics Department, University of Utah, 155 S 1400 E RM 233, Salt Lake City UT 84112-0090 (fguevara@math.utah.edu, mauck@math.utah.edu).

[1]Herglotz wave functions may also be defined as integrals over $S(0,1)$, see e.g. [2, §3].

taking $\phi = \vec{\boldsymbol{n}} \cdot \nabla v + ik\alpha v$ gives a function $v$ solving (2) whose nodal set is close to the desired pattern.

**1.1. Related work.** The forces that a standing acoustic field in a fluid exerts on compressible particles can be described by an acoustic radiation potential [10, 18, 6, 15], whose minima correspond to locations where the particles tend to cluster. The results we present here apply only to the case where the minima coincide with the zero level set of the wave field, e.g. when the particles are less compressible than the fluid and are neutrally buoyant in the fluid. The problem of designing Helmholtz equation solutions for which the minima of the acoustic radiation potential are close to a desired pattern has been studied numerically and experimentally in both 2D and 3D settings [8, 14]. The numerical approach in [8, 14] allows for a broader range of particle and fluid parameters than the one we consider here and also accounts for having finitely many transducers lining the reservoir. The design problem is formulated as a constrained minimization problem in [8]. The objective function is a quadratic functional representing an aggregate of the acoustic radiation potential at the points where particles are desired. A quadratic constraint restricts the minimization to transducer excitations with the same total power. The minimization can be solved efficiently as it is equivalent to finding the eigenvector corresponding to the smallest (algebraically speaking) eigenvalue of a matrix [8].

We emphasize that we are interested in approximating functions that are not necessarily Helmholtz equation solutions with Herglotz wave functions. Thus, the problem we consider here is fundamentally different from the results showing that Herglotz wave functions are dense in the space of solutions to the Helmholtz equation [17]. Another related problem is that of approximating an entire solution to the Helmholtz equation in a region by a linear combination of singular Helmholtz equation solutions. This can be done using Green's identities (see e.g. [2]) and has applications to active cloaking as proposed in [11]. Indeed, such an approximation scheme could be used to significantly reduce an incident field within a region, which in turn suppresses scattering from any object that we wish to hide within the region. Other approaches to solve the same problem, while not completely surrounding the object with sources, include [9, 12].

**1.2. Contents.** We first consider the approximation problem on a ball of radius $R$ in section 2. The solution to this problem is related to a time reversal experiment where the source density is the function we wish to approximate. When the approximation problem is restricted to a plane (section 3), the best approximation is not related to time reversal but is a low pass filtered version of the function we wish to approximate. We illustrate both approaches with numerical experiments in section 4 and conclude with a summary and future work in section 5.

**2. Approximation by Herglotz wave functions restricted to a ball.** In section 2.1 we give a heuristic that motivates the best approximation result we are after. Some facts about time reversal are recalled in section 2.2 and its connection with the heuristic is in section 2.3. For the best approximation result, we work on a space of Herglotz wave functions restricted to the ball $B(0, R)$, which is defined and studied in section 2.4. The projection of a function into this space is carried out in section 2.5. Finally we explain in section 2.6 how the projection and the heuristic are related.

**2.1. A motivating heuristic.** Let $u$ be a solution to the Helmholtz equation with wavenumber $k$. If the Fourier transform $\widehat{u}(\vec{\boldsymbol{\xi}})$ of $u$ is well-defined (perhaps in the

sense of distributions), it must satisfy

$$(-|\vec{\boldsymbol{\xi}}|^2 + k^2)\widehat{u}(\vec{\boldsymbol{\xi}}) = 0. \tag{3}$$

In particular we must have $\operatorname{supp}\widehat{u} \subset S(0,k)$. Thus if we are given a function $f$ to approximate with a Helmholtz equation solution, it would make sense to use as approximation a function $g$ whose Fourier transform $\widehat{g}(\vec{\boldsymbol{\xi}})$ coincides with $\widehat{f}(\vec{\boldsymbol{\xi}})$ on the sphere $|\vec{\boldsymbol{\xi}}| = k$, but is zero elsewhere. This heuristic of "filtering out everything outside of $S(0,k)$ in spatial frequency" sets the expectations for the approximation result we are after. First we need to use appropriate spaces to be able to compare a function defined on some subset of $\mathbb{R}^3$ with functions defined on a sphere. Second, the approximation can be very poor, since a function with zero Fourier transform on the sphere $|\vec{\boldsymbol{\xi}}| = k$ but non-zero elsewhere would be approximated by the zero solution to the Helmholtz equation.

**2.2. Time reversal and convolution with a spherical Bessel function.** *Time reversal* consists in recording an acoustic field at a surface (the time reversal mirror), time reversing it and propagating it back in the medium [4]. The field at location $\vec{\boldsymbol{x}}$ generated by a point source in a homogeneous medium at location $\vec{\boldsymbol{y}}$ is $G(\vec{\boldsymbol{x}} - \vec{\boldsymbol{y}}, k)$, where $G$ is the free space Green function for the Helmholtz equation

$$G(\vec{\boldsymbol{x}}, k) = \frac{\exp[ik|\vec{\boldsymbol{x}}|]}{4\pi|\vec{\boldsymbol{x}}|}. \tag{4}$$

The time reversal procedure applied to the field $G(\vec{\boldsymbol{x}} - \vec{\boldsymbol{y}}, k)$, with time reversal mirror being the sphere $S(0,R)$, gives the field

$$u_{\vec{\boldsymbol{y}}}(\vec{\boldsymbol{x}}) = \int_{S(0,R)} G(\vec{\boldsymbol{x}} - \vec{\boldsymbol{z}}, k)\overline{G(\vec{\boldsymbol{z}} - \vec{\boldsymbol{y}}, k)}dS(\vec{\boldsymbol{z}}) = \frac{1}{k}\operatorname{Im} G(\vec{\boldsymbol{x}} - \vec{\boldsymbol{y}}, k), \tag{5}$$

assuming the source is inside the sphere, i.e. $|\vec{\boldsymbol{y}}| < R$. This follows from the Helmholtz-Kirchhoff identity [5, §2.1]. Thus the imaginary part of the Green function gives the tightest possible spot that can be focused using waves in a homogeneous medium at wavenumber $k$. Using (4) and the zero-th order spherical Bessel function $j_0(t) = \sin(t)/t$ we get that

$$u_{\vec{\boldsymbol{y}}}(\vec{\boldsymbol{x}}) = (4\pi)^{-1} j_0(k|\vec{\boldsymbol{x}} - \vec{\boldsymbol{y}}|).$$

The same principle can be applied to more complicated source densities. If $f$ is an $L^\infty$ real valued source density function with $\operatorname{supp} f \subset B(0,R)$, the resulting field is $G(\cdot,k) * f$ and time reversing it with a time reversal mirror on $S(0,R)$ gives $(4\pi)^{-1} j_0(k|\cdot|) * f$. Hence time reversal and convolution with $(4\pi)^{-1} j_0(k|\cdot|)$ are equivalent in this setting.

**2.3. Convolution with a spherical Bessel function and the heuristic.** As we see in the next lemma, convolution with $j_0(k|\cdot|)$ (and thus time reversal) is equivalent (up to a multiplicative constant) to the heuristic of "filtering everything outside of $S(0,k)$ in spatial frequency".

LEMMA 1. *Let $f$ be a compactly supported $L^\infty$ function, then*

$$[f * j_0(k|\cdot|)](\vec{\boldsymbol{x}}) = \frac{1}{4\pi k^2}\int_{S(0,k)} \widehat{f}(\vec{\boldsymbol{z}}) \exp[i\vec{\boldsymbol{x}} \cdot \vec{\boldsymbol{z}}] dS(\vec{\boldsymbol{z}}). \tag{6}$$

*In other words, $f * j_0(k|\cdot|)$ is a Herglotz wave function with wavenumber $k$ and density $\widehat{f}(\vec{\boldsymbol{z}})|_{S(0,k)}/(4\pi k^2)$.*

*Proof.* By the Funk-Hecke formula (see e.g. [2, §2.4]), we have that

$$j_0(k|\vec{\boldsymbol{x}}|) = \frac{1}{4\pi k^2}\int_{S(0,k)} \exp[i\vec{\boldsymbol{x}}\cdot\vec{\boldsymbol{z}}]dS(\vec{\boldsymbol{z}}). \tag{7}$$

Using the previous expression for $j_0(k|\cdot|)$ in the convolution gives the desired result:

$$\begin{aligned}(f * j_0(k|\cdot|))(\vec{\boldsymbol{x}}) &= \frac{1}{4\pi k^2}\int d\vec{\boldsymbol{y}}\, f(\vec{\boldsymbol{y}})\int_{S(0,k)} dS(\vec{\boldsymbol{z}})\exp[i(\vec{\boldsymbol{x}}-\vec{\boldsymbol{y}})\cdot\vec{\boldsymbol{z}}]\\ &= \frac{1}{4\pi k^2}\int_{S(0,k)} dS(\vec{\boldsymbol{z}})\,\exp[i\vec{\boldsymbol{x}}\cdot\vec{\boldsymbol{z}}]\int d\vec{\boldsymbol{y}}\,\exp[-i\vec{\boldsymbol{y}}\cdot\vec{\boldsymbol{z}}]f(\vec{\boldsymbol{y}})\\ &= \frac{1}{4\pi k^2}\int_{S(0,k)} dS(\vec{\boldsymbol{z}})\,\exp[i\vec{\boldsymbol{x}}\cdot\vec{\boldsymbol{z}}]\widehat{f}(\vec{\boldsymbol{z}}).\end{aligned}$$

We point out that $\widehat{f}$ is $C^\infty$ by the Paley-Wiener theorem since $f$ is compactly supported. ∎

**2.4. Herglotz wave functions restricted to a ball.** Let us consider the family of spherical wave functions

$$u_{nm}(\vec{\boldsymbol{x}}) = j_n(k|\vec{\boldsymbol{x}}|)Y_{nm}(\vec{\boldsymbol{x}}/|\vec{\boldsymbol{x}}|), n = 0,1,\dots, m = -n,\dots n, \tag{8}$$

where the $Y_{nm}$ are spherical harmonics defined as in [2] and normalized to be orthonormal in $L^2(S(0,1))$. The $u_{nm}$ are solutions to the Helmholtz equation and by the Funk-Hecke formula they are also Herglotz wave functions [2, §2.4]. Indeed we have for $n = 0,1,\dots, m = -n,\dots n$ that

$$u_{nm}(\vec{\boldsymbol{x}}) = \frac{i^n}{4\pi k^2}\int_{S(0,k)} \exp[i\vec{\boldsymbol{x}}\cdot\vec{\boldsymbol{z}}]Y_{nm}(\vec{\boldsymbol{z}}/k)dS(\vec{\boldsymbol{z}}). \tag{9}$$

We consider the $(N+1)^2$ dimensional space of Herglotz wave functions

$$S_{R,N} \equiv \operatorname{span}\left\{u_{nm}|_{B(0,R)},\ n = 0,\dots,N,\ m = -n,\dots n\right\}. \tag{10}$$

The orthogonality of the spherical harmonics $Y_{nm}$ with respect to the $L^2(S(0,1))$ inner product guarantees that the spherical wave functions $u_{nm}$ (with order up to $N$) form an orthogonal basis of $S_{R,N}$ with respect to the $L^2(B(0,R))$ inner product. The next lemma shows that we can, for all practical purposes, think of the functions $(k\sqrt{2}/R)u_{nm}$ as an *orthonormal* basis for $S_{R,N}$ provided $R$ is sufficiently large.

LEMMA 2. *As $R\to\infty$ and for $N$ fixed, the spherical wave functions for $n = 0,\dots,N$ and $m = -n,\dots,n$ satisfy*

$$\frac{2k^2}{R}\|u_{nm}\|^2_{L^2(B(0,R))} \to 1.$$

*Proof.* The norm of a spherical wave function $u_{nm}$ restricted to the ball $B(0,R)$ is

$$\|u_{nm}\|^2_{L^2(B(0,R))} = \int_0^R r^2[j_n(kr)]^2\,dr = \frac{1}{k^3}\int_0^{kR} t^2[j_n(t)]^2\,dt.$$

Using the asymptotic (see e.g. [2, §3.3])

$$\lim_{T\to\infty}\frac{1}{T}\int_0^T r^2[j_n(r)]^2 dr = \frac{1}{2},$$

we see that $R^{-1}\|u_{nm}\|^2_{L^2(B(0,R))} \to (2k^2)^{-1}$ as $R\to\infty$ and $N$ is kept fixed. ∎

**2.5. Projection onto a space of restricted Herglotz wave functions.** Let $f$ be an $L^\infty$ function with compact support $D$ and assume $R$ is large enough so that $D \subset B(0,R)$. Then clearly $f \in L^2(B(0,R))$ and the best approximation $f_{R,N}$ of $f$ by functions in $S_{R,N}$ is given by its orthogonal projection:

$$f_{R,N} = \sum_{n=0}^{N} \sum_{m=-n}^{n} \frac{\langle u_{nm}, f\rangle}{\langle u_{nm}, u_{nm}\rangle} u_{nm}, \tag{11}$$

where $\langle \cdot, \cdot \rangle$ is the inner product on $L^2(B(0,R))$. The inner products $\langle u_{nm}, f\rangle$ measure spherical harmonic coefficients of $\widehat{f}$ on the sphere $S(0,k)$, as we show next.

LEMMA 3. *Let $f$ be an $L^\infty$ function with* $\operatorname{supp} f \subset B(0,R)$. *Then we have*

$$\langle u_{nm}, f\rangle_{L^2(B(0,R))} = (4\pi i^n k^2)^{-1} \langle Y_{nm}(\cdot/k), \widehat{f}\rangle_{L^2(S(0,k))}.$$

*Proof.* Writing the $L^2(B(0,R))$ inner product and using the Funk-Hecke formula (9) we get

$$\begin{aligned}
\langle u_{nm}, f\rangle_{L^2(B(0,R))} &= \frac{1}{4\pi k^2 i^n} \int_{B(0,R)} d\vec{\boldsymbol{x}}\, f(\vec{\boldsymbol{x}}) \left[ \int_{S(0,k)} dS(\vec{\boldsymbol{z}}) \exp[-i\vec{\boldsymbol{x}} \cdot \vec{\boldsymbol{z}}] \overline{Y}_{nm}(\vec{\boldsymbol{z}}/k) \right] \\
&= \frac{1}{4\pi k^2 i^n} \int_{S(0,k)} dS(\vec{\boldsymbol{z}})\, \overline{Y}_{nm}(\vec{\boldsymbol{z}}/k) \int_{B(0,R)} d\vec{\boldsymbol{x}} f(\vec{\boldsymbol{x}}) \exp[-i\vec{\boldsymbol{x}} \cdot \vec{\boldsymbol{z}}] \\
&= \frac{1}{4\pi k^2 i^n} \int_{S(0,k)} dS(\vec{\boldsymbol{z}})\, \overline{Y}_{nm}(\vec{\boldsymbol{z}}/k) \widehat{f}(\vec{\boldsymbol{z}}),
\end{aligned}$$

which proves the desired result. ∎

The best approximation $f_{R,N}$ is a Herglotz wave function on $S(0,k)$. Its density is given in the next lemma.

LEMMA 4. *The best approximation $f_{R,N}$ in (11) can be written as a Herglotz wave function on $S(0,k)$ with density*

$$g_{R,N}(\vec{\boldsymbol{z}}) = \frac{1}{(4\pi k^2)^2} \sum_{n=0}^{N} \sum_{m=-n}^{n} \frac{\langle Y_{nm}(\cdot/k), \widehat{f}\rangle_{L^2(S(0,k))}}{\langle u_{nm}, u_{nm}\rangle_{L^2(B(0,R))}} Y_{nm}(\vec{\boldsymbol{z}}/k). \tag{12}$$

*Proof.* In the definition (11) of $f_{R,N}$ we use the Funk-Hecke formula (9) to replace the right-most $u_{nm}$ and get

$$\begin{aligned}
f_{R,N}(\vec{\boldsymbol{x}}) &= \sum_{n=0}^{N} \sum_{m=-n}^{n} \frac{\langle u_{nm}, f\rangle}{\langle u_{nm}, u_{nm}\rangle} \frac{i^n}{4\pi k^2} \int_{S(0,k)} \exp[i\vec{\boldsymbol{z}} \cdot \vec{\boldsymbol{x}}] Y_{nm}(\vec{\boldsymbol{z}}/k) dS(\vec{\boldsymbol{z}}) \\
&= \int_{S(0,k)} \exp[i\vec{\boldsymbol{z}} \cdot \vec{\boldsymbol{x}}] g_{R,N}(\vec{\boldsymbol{z}}) dS(\vec{\boldsymbol{z}}),
\end{aligned}$$

where $g_{R,N}(\vec{\boldsymbol{z}})$ is given for $\vec{\boldsymbol{z}} \in S(0,k)$ by

$$\begin{aligned}
g_{R,N}(\vec{\boldsymbol{z}}) &= \sum_{n=0}^{N} \sum_{m=-n}^{n} \frac{\langle u_{nm}, f\rangle}{\langle u_{nm}, u_{nm}\rangle} \frac{i^n}{4\pi k^2} Y_{nm}(\vec{\boldsymbol{z}}/k) \\
&= \frac{1}{(4\pi k^2)^2} \sum_{n=0}^{N} \sum_{m=-n}^{n} \frac{\langle Y_{nm}(\cdot/k), \widehat{f}\rangle_{L^2(S(0,k))}}{\langle u_{nm}, u_{nm}\rangle_{L^2(B(0,R))}} Y_{nm}(\vec{\boldsymbol{z}}/k),
\end{aligned}$$

where we used Lemma 3 for the second equality. ∎

**2.6. Relation between projection and heuristic.** We now use the $R$ large asymptotic result for $\|u_{nm}\|_{L^2(B(0,R))}$ to show that the Herglotz density of the best approximation $f_{R,N}$ approaches that of the projection of $\widehat{f}$ onto the spherical harmonics up to order $N$ in $S(0,k)$. This shows that the heuristic of filtering out everything outside of the sphere $S(0,k)$ in spatial frequency is related to approximating a function by Herglotz wave functions. Note that we need to work in $L^2(B(0,R))$ because entire solutions to the Helmholtz equation are not in $L^2(B(0,R))$ (because of their growth at infinity, see e.g. [2, §3.3]).

THEOREM 5. *Let $g_{R,N}$ be the Herglotz density on $S(0,k)$ defined in (12). Then for a fixed $N$ we have as $R \to \infty$*

$$8\pi^2 R g_{R,N} \to \sum_{n=0}^{N} \sum_{m=-n}^{n} \langle k^{-1} Y_{nm}(\cdot/k), \widehat{f} \rangle_{L^2(S(0,k))} k^{-1} Y_{nm}(\cdot/k),$$

*where the convergence is understood in $L^2(S(0,k))$ and the limiting function is the projection of $\widehat{f}$ onto the spherical harmonic basis of $S(0,k)$ up to order $N$.*

*Proof.* We recall that the functions $k^{-1}Y_{nm}(\cdot/k)$ form an orthonormal basis of $L^2(S(0,k))$. By Lemma 4, the coefficient of $8\pi^2 R g_{R,N}$ along the basis function $k^{-1}Y_{nm}(\cdot/k)$ is

$$\langle k^{-1} Y_{nm}(\cdot/k), 8\pi^2 R g_{R,N} \rangle_{L^2(S(0,k))} = \frac{R}{2k^2} \frac{\langle k^{-1} Y_{nm}(\cdot/k), \widehat{f} \rangle_{L^2(S(0,k))}}{\langle u_{nm}, u_{nm} \rangle_{L^2(B(0,R))}}.$$

Using Lemma 2 we get that as $R \to \infty$,

$$\langle k^{-1} Y_{nm}(\cdot/k), 8\pi^2 R g_{R,N} \rangle_{L^2(S(0,k))} \to \langle k^{-1} Y_{nm}(\cdot/k), \widehat{f} \rangle_{L^2(S(0,k))}.$$

This shows the desired result. ∎

**3. Approximation by Herglotz wave functions restricted to a plane.** We would like to find a Herglotz wave function whose restriction to a plane is as close as possible to a function defined on the same plane. To study this problem we introduce a weighted space of Herglotz wave functions (section 3.1) and also a space of band-limited functions (section 3.2). We establish a one-to-one correspondence between these spaces and use this fact to find the best approximation of a function in $L^2(\mathbb{R}^2)$ by a Herglotz wave function restricted to a plane (section 3.3). Since time reversal can be used to express the solution to the best approximation by Herglotz wave functions in a volume (section 2), we apply the same principle to approximate a function defined on a plane and show that the time reversal solution is suboptimal (section 3.4). The final result is that the approximation problem we consider is (up to multiplicative constants) equivalent to filtering out all the spatial frequencies $\boldsymbol{\xi}$ such that $|\boldsymbol{\xi}| > k$ in the function we want to approximate. This limits the resolution that is achievable by this approach to about a wavelength, which is consistent with the Rayleigh resolution limit for imaging with waves (see e.g. [1]). To see this, consider the distribution $\delta(\boldsymbol{x})$. Filtering out all the spatial frequencies of $\delta(\boldsymbol{x})$ outside of $B(0,k)$ gives the function

$$(\chi_{B(0,k)})^{\vee}(\boldsymbol{x}) = (2\pi)^{-1} \frac{J_1(k|\boldsymbol{x}|)}{|\boldsymbol{x}|},$$

where $\vee$ denotes the inverse Fourier transform. The first zero of $J_1(kz)/z$ is located at $z \approx 1.22\lambda/2$ (see e.g. [3, §10]), thus the smallest feature we can resolve is about $1.22\lambda$. Hereinafter, vectors $\vec{\boldsymbol{x}} \in \mathbb{R}^3$ have arrows and the first two components of $\vec{\boldsymbol{x}} \in \mathbb{R}^3$ are denoted by $\boldsymbol{x} \in \mathbb{R}^2$, i.e. we have $\vec{\boldsymbol{x}} = (\boldsymbol{x}, x_3)$.

**3.1. A weighted space of Herglotz wave functions.** For a given wavenumber $k$, let us define the space $S_k$ of Herglotz wave functions with density in a weighted $L^2$ space on the sphere of radius $k$:

$$S_k = \left\{ \int_{S(0,k)} g(\vec{\boldsymbol{z}}) e^{i\vec{\boldsymbol{z}}\cdot\vec{\boldsymbol{x}}} dS(\vec{\boldsymbol{z}}) \mid g \in L^2_W(S(0,k)) \right\}, \tag{13}$$

where $g \in L^2_W(S(0,k))$ if and only if

$$\int_{S(0,k)} \frac{|g(\vec{\boldsymbol{z}})|^2}{|z_3|} dS(\vec{\boldsymbol{z}}) < \infty.$$

Naturally, we need to make sure that the integral in the definition of a function in $S_k$ is well defined. This follows from the Cauchy-Schwartz inequality:

$$\begin{aligned} \int_{S(0,k)} g(\vec{\boldsymbol{z}}) e^{i\vec{\boldsymbol{z}}\cdot\vec{\boldsymbol{x}}} dS(\vec{\boldsymbol{z}}) &= \int_{S(0,k)} \frac{g(\vec{\boldsymbol{z}})}{|z_3|^{1/2}} |z_3|^{1/2} e^{i\vec{\boldsymbol{z}}\cdot\vec{\boldsymbol{x}}} dS(\vec{\boldsymbol{z}}) \\ &\leq \left[ \int_{S(0,k)} \frac{|g(\vec{\boldsymbol{z}})|^2}{|z_3|} dS(\vec{\boldsymbol{z}}) \right]^{1/2} \left[ \int_{S(0,k)} |z_3| dS(\vec{\boldsymbol{z}}) \right]^{1/2}, \end{aligned}$$

where the upper bound is finite when $g \in L^2_W(S(0,k))$.

**3.2. Relation between Herglotz wave functions and band-limited functions.** For the wavenumber $k$, we define the space of band-limited functions

$$B_k = \{ f \in L^2(\mathbb{R}^2) \mid \operatorname{supp} \widehat{f} \subset B(0,k) \}, \tag{14}$$

where $B(0,k)$ is the ball of radius $k$ centered at the origin. In the next lemma, we show that $B_k$ can be identified with the space of restrictions of elements of $S_k$ to the plane $x_3 = 0$. In fact we only need to consider the subset $S_{k+}$ of $S_k$ consisting of Herglotz wave functions with density $g \in L^2_W(S(0,k))$, supported on the half sphere $\{\vec{\boldsymbol{z}} \mid \vec{\boldsymbol{z}} \in S(0,k), z_3 \geq 0\}$.

LEMMA 6. *Let $u \in S_{k+}$, then the function $f : \boldsymbol{x} \to u(\boldsymbol{x}, 0)$ is a function in $B_k$. Conversely for any function $f \in B_k$, there is a Herglotz wave function $u \in S_{k+}$ such that $f(\boldsymbol{x}) = u(\boldsymbol{x}, 0)$.*

*Proof.* Let $u \in S_{k+}$ and let $g$ be its density. Restricting $u$ to the plane $x_3 = 0$, we get

$$\begin{aligned} u(\boldsymbol{x}, 0) &= \int_{S(0,k), z_3 \geq 0} g(\vec{\boldsymbol{z}}) e^{i(\boldsymbol{z}, z_3)\cdot(\boldsymbol{x}, 0)} dS(\vec{\boldsymbol{z}}) \\ &= \int_{B(0,k)} g(\boldsymbol{z}, \sqrt{k^2 - |\boldsymbol{z}|^2}) e^{i\boldsymbol{z}\cdot\boldsymbol{x}} \frac{k}{\sqrt{k^2 - |\boldsymbol{z}|^2}} d\boldsymbol{z}. \end{aligned}$$

Therefore $u(\boldsymbol{x}, 0)$ is the Fourier transform of the $L^2(B(0,k))$ function

$$v(\boldsymbol{z}) = (2\pi)^2 g(\boldsymbol{z}, \sqrt{k^2 - |\boldsymbol{z}|^2}) \frac{k}{\sqrt{k^2 - |\boldsymbol{z}|^2}} \chi_{B(0,k)}(\boldsymbol{z}), \tag{15}$$

and $u(\boldsymbol{x},0) \in B_k$. Indeed we have

$$\begin{aligned}\int_{B(0,k)} |v(\boldsymbol{z})|^2 d\boldsymbol{z} &= (2\pi)^4 k^2 \int_{B(0,k)} \left| \frac{g(\boldsymbol{z}, \sqrt{k^2-|\boldsymbol{z}|^2})}{\sqrt{k^2-|\boldsymbol{z}|^2}} \right|^2 d\boldsymbol{z} \\ &= (2\pi)^4 k^2 \int_{S(0,k), z_3 \geq 0} \frac{|g(\vec{\boldsymbol{z}})|^2}{z_3^2} \frac{\sqrt{k^2-|\boldsymbol{z}|^2}}{k} dS(\vec{\boldsymbol{z}}) \\ &= (2\pi)^4 k \int_{S(0,k), z_3 \geq 0} \frac{|g(\vec{\boldsymbol{z}})|^2}{z_3} dS(\vec{\boldsymbol{z}}) < \infty.\end{aligned}$$

Now take a function $f \in B_k$. Since $\widehat{f}$ is supported in $B(0,k)$ we have

$$\begin{aligned}f(\boldsymbol{x}) &= (2\pi)^{-2} \int_{B(0,k)} \widehat{f}(\boldsymbol{z}) e^{i\boldsymbol{z}\cdot\boldsymbol{x}} d\boldsymbol{z} \\ &= (2\pi)^{-2} \int_{S(0,k), z_3 \geq 0} \widehat{f}(\boldsymbol{z}) e^{i(\boldsymbol{z},z_3)\cdot(\boldsymbol{x},0)} \frac{\sqrt{k^2-|\boldsymbol{z}|^2}}{k} dS(\vec{\boldsymbol{z}}).\end{aligned}$$

Thus $f(\boldsymbol{x})$ is the restriction to the plane $x_3 = 0$ of a Herglotz wave function with density

$$g(\vec{\boldsymbol{z}}) = (2\pi)^{-2} \widehat{f}(\boldsymbol{z}) \frac{\sqrt{k^2-|\boldsymbol{z}|^2}}{k} \chi_{z_3 \geq 0}(\vec{\boldsymbol{z}}) = (2\pi)^{-2} \widehat{f}(\boldsymbol{z}) \frac{(z_3)_+}{k},$$

where $x_+ \equiv (x+|x|)/2$. Notice $g \in L^2_W(S(0,k))$ because

$$\begin{aligned}\int_{S(0,k)} \frac{|g(\vec{\boldsymbol{z}})|^2}{|z_3|} dS(\vec{\boldsymbol{z}}) &= \frac{(2\pi)^{-4}}{k^2} \int_{S(0,k), z_3 \geq 0} \frac{|\widehat{f}(\boldsymbol{z})(z_3)_+|^2}{|z_3|} dS(\vec{\boldsymbol{z}}) \\ &= \frac{(2\pi)^{-4}}{k} \int_{B(0,k)} |\widehat{f}(\boldsymbol{z})|^2 d\boldsymbol{z} < \infty.\end{aligned}$$

∎

**3.3. Best approximation by Herglotz wave functions restricted to a plane.** Here we use the one-to-one relationship between elements of $B_k$ and elements of $S_{k+}|_{x_3=0}$ to find the best approximation of a function $f \in L^2(\mathbb{R}^2)$ by a Herglotz wave function in $S_{k+}|_{x_3=0}$. Furthermore, we show that there is nothing to gain if we consider Herglotz wave functions supported over all of $S(0,k)$, instead of only supported on the upper half sphere, that is replacing $S_{k+}$ by $S_k$.

THEOREM 7. *Let $f \in L^2(\mathbb{R}^2)$. The best approximation of $f$ by a Herglotz wave function in $S_{k+}$ restricted to the plane $x_3 = 0$ has density*

$$g(\vec{\boldsymbol{z}}) = (2\pi)^{-2} \chi_{B(0,k)}(\boldsymbol{z}) \widehat{f}(\boldsymbol{z}) \frac{(z_3)_+}{k}, \text{ with } |\vec{\boldsymbol{z}}| = k. \tag{16}$$

*Proof.* In operator notation, the orthogonal projection onto $B_k$ is $\mathcal{F}^{-1}\mathcal{B}_k\mathcal{F}$, where $\mathcal{F}$ is the Fourier transform operator and $\mathcal{B}_k$ is the operator of multiplication by the function $\chi_{B(0,k)}$. That this is indeed an orthogonal projector can be easily verified, see e.g. [16]. Therefore the best approximation of $f$ by a function in $B_k$ is $\tilde{f} = \mathcal{F}^{-1}\mathcal{B}_k\mathcal{F}f$. By Lemma 6, $\tilde{f}$ can be identified with the restriction to the plane $x_3 = 0$ of some Herglotz wave function in $S_{k+}$ with density being (16). It follows from the proof of Lemma 6 that $g \in L^2_W(S(0,k))$. Indeed $\widehat{f} \in L^2(\mathbb{R}^2)$ implies that $\chi_{B(0,k)}\widehat{f} \in L^2(B(0,k))$. ∎

A natural question to ask is whether we get a better approximation if we approximate with all the Herglotz wave functions in $S_k$, instead of limiting ourselves to $S_{k+}$. The approximation we get in Theorem 7 with functions in $S_{k+}$ is already optimal, as we show next.

COROLLARY 8. *Let $f \in L^2(\mathbb{R}^2)$. The best approximation of $f$ by a Herglotz wave function in $S_k$ restricted to the plane $x_3 = 0$ has density (16) on the sphere $|\vec{\boldsymbol{z}}| = k$.*

*Proof.* We show that the space of functions obtained by restricting $S_k$ to the plane $x_3 = 0$ is $B_k$, i.e. identical to that obtained by restricting $S_{k+}$. For a $u \in S_k$ with density $g(\vec{\boldsymbol{z}})$ we have

$$\begin{aligned} u(\vec{\boldsymbol{x}}) &= \int_{S(0,k)} e^{i\vec{\boldsymbol{x}}\cdot\vec{\boldsymbol{z}}} g(\vec{\boldsymbol{z}}) dS(\vec{\boldsymbol{z}}) \\ &= \int_{S(0,k),z_3>0} [e^{i\vec{\boldsymbol{x}}\cdot(\boldsymbol{z},z_3)} g_+(\vec{\boldsymbol{z}}) + e^{i\vec{\boldsymbol{x}}\cdot(\boldsymbol{z},-z_3)} g_-(\vec{\boldsymbol{z}})] dS(\vec{\boldsymbol{z}}), \end{aligned}$$

where $g_+(\vec{\boldsymbol{z}}) = g(\boldsymbol{z}, z_3)$ and $g_-(\vec{\boldsymbol{z}}) = g(\boldsymbol{z}, -z_3)$. Restricting $u$ to the plane $x_3 = 0$ we get

$$u(\boldsymbol{x}, 0) = \int_{S(0,k),z_3>0} e^{i\boldsymbol{x}\cdot\boldsymbol{z}} [g_+(\vec{\boldsymbol{z}}) + g_-(\vec{\boldsymbol{z}})] dS(\vec{\boldsymbol{z}}).$$

Clearly $g_+$ and $g_-$ are in $L^2_W(S(0,k))$, hence we have that $u(\boldsymbol{x}, 0) \in B_k$. ∎

**3.4. Does time reversal solve the approximation problem?.** In section 2.2 we saw that time reversal of a volumetric source distribution $f$ is equivalent to convolution with $(4\pi)^{-1} j_0(k|\cdot|)$ and is related to the best approximation in a ball (section 2). For functions that are supported on the plane $x_3 = 0$, we show in Theorem 9 that convolution with $j_0(k|\cdot|)$ is a filter with spatial frequency response supported on $B(0,k)$, as the filter we obtained in section 3.3 but suboptimal.

THEOREM 9. *Let $f \in L^2(\mathbb{R}^2)$ be such that*

$$\int_{B(0,k)} \frac{|\widehat{f}(\boldsymbol{\xi})|^2}{k^2 - |\boldsymbol{\xi}|^2} d\boldsymbol{\xi} < \infty.$$

*Time reversal of point sources modulated by $f$ and located on the plane $x_3 = 0$ gives the Helmholtz equation solution $u(\vec{\boldsymbol{x}}) = (j_0(k|\cdot|) * f)(\vec{\boldsymbol{x}})$, where the convolution is over $x_1, x_2$. The restriction of $u(\vec{\boldsymbol{x}})$ to the plane $x_3 = 0$ has Fourier transform*

$$(u(\boldsymbol{x}, 0))^\wedge = \frac{2\pi}{k\sqrt{k^2 - |\boldsymbol{\xi}|^2}} \widehat{f}(\boldsymbol{\xi}) \chi_{B(0,k)}(\boldsymbol{\xi}).$$

*Moreover, $u(\vec{\boldsymbol{x}})$ is a Herglotz wave function with density*

$$g(\vec{\boldsymbol{z}}) = (2\pi)^{-1} k^{-2} \widehat{f}(\boldsymbol{z}) \chi_{z_3>0}(\vec{\boldsymbol{z}}),$$

*on the sphere $|\vec{\boldsymbol{z}}| = k$.*

*Proof.* From the Funk-Hecke formula (see e.g. [2, §2.4]), we get

$$j_0(k|\vec{\boldsymbol{x}}|) = \frac{1}{4\pi k^2} \int_{S(0,k)} e^{i\vec{\boldsymbol{z}}\cdot\vec{\boldsymbol{x}}} dS(\vec{\boldsymbol{z}}), \tag{17}$$

and thus $j_0(k|\vec{\boldsymbol{x}}|)$ is a Herglotz wave function with constant density $1/(4\pi k^2)$ on $S(0,k)$. The restriction $j_0(k|\boldsymbol{x}|) = j_0(k|(\boldsymbol{x},0)|)$ of $j_0(k|\vec{\boldsymbol{x}}|)$ to the plane $x_3 = 0$ is

$$j_0(k|\boldsymbol{x}|) = \frac{1}{4\pi k^2}\int_{S(0,k)} e^{i\boldsymbol{z}\cdot\boldsymbol{x}} dS(\vec{\boldsymbol{z}}) = \frac{1}{2\pi k^2}\int_{S(0,k),z_3>0} e^{i\boldsymbol{z}\cdot\boldsymbol{x}} dS(\vec{\boldsymbol{z}}),$$

where the last equality comes from changing variables in the lower half sphere. By a reasoning similar to the proof of Lemma 6, the Fourier transform of $j_0(k|\boldsymbol{x}|)$ as a function on $\mathbb{R}^2$ is:

$$[j_0(k|\cdot|)]^\wedge(\boldsymbol{\xi}) = \frac{2\pi}{k\sqrt{k^2-|\boldsymbol{\xi}|^2}}\chi_{B(0,k)}(\boldsymbol{\xi}).$$

In the frequency domain the convolution becomes

$$\begin{aligned}(j_0(k|\cdot|) * f)^\wedge(\boldsymbol{\xi}) &= [j_0(k|\cdot|)]^\wedge(\boldsymbol{\xi})\widehat{f}(\boldsymbol{\xi}) \\ &= \frac{2\pi}{k\sqrt{k^2-|\boldsymbol{\xi}|^2}}\widehat{f}(\boldsymbol{\xi})\chi_{B(0,k)}(\boldsymbol{\xi}).\end{aligned}$$

Hence the hypothesis on $f$ guarantees that $j_0(k|\cdot|) * f \in B_k$. By Lemma 6, we know that $j_0(k|\cdot|) * f$ is a Herglotz wave function with bounded density supported on the half sphere $\{\vec{\boldsymbol{z}} \mid \vec{\boldsymbol{z}} \in S(0,k), z_3 \geq 0\}$. Its density can be obtained using Theorem 7. ∎

**4. Numerical experiments.** We saw in section 2 that the best approximation of a function $f$ by Herglotz wave functions is essentially given by keeping only the Fourier components of $f$ that lie on the sphere $S(0,k)$. We illustrate this procedure with numerical experiments in section 4.1, where as expected we get poor approximations of the function $f$ in a volume. When the goal is to approximate a function in the plane by Herglotz wave functions restricted to the same plane, we saw in section 3 that we can expect the approximation to be a low pass filtered version of the function we wish to approximate. We illustrate this procedure and compare it to time reversal in section 4.2.

**4.1. Approximation on a volume.** We recall from section 2 that the best approximation of a function by spherical wave functions on a ball of radius $R$ is a Herglotz wave function with density given by (12). Instead of calculating (12), we use the asymptotic result in Theorem 5 which shows that the density (12) approaches $\widehat{f}|_{S(0,k)}$ in some sense. We approximate the Herglotz wave function with density $\widehat{f}|_{S(0,k)}$ as follows.

Step 1. Discretize the sphere $S(0,k)$ with a Delaunay triangulation.

Step 2. Use a uniform spatial grid to discretize $f$ on a cube. Using the DFT, this gives an approximation to $\widehat{f}$ on a uniform (spatial) frequency grid.

Step 3. Approximate $\widehat{f}$ at the triangle centers of the triangulation of $S(0,k)$ by linearly interpolating the $\widehat{f}$ calculated in Step 2.

Step 4. The Herglotz wave function $u$ with density $\widehat{f}$ is given by the integral (1) with $g \equiv \widehat{f}$, that we approximate by assuming it is piecewise constant on the triangles of the triangulation of $S(0,k)$. Thus $u$ is approximated by a finite sum of plane waves with wavenumber $k$.

We illustrate this procedure in Figure 1, with a function $f$ that is related to a tetrahedron $T$ with center of mass at the origin and circumscribing sphere of radius $5\lambda$ and is given by

$$f(\vec{\boldsymbol{x}}) = |T|\chi_{B(0,5\lambda)}(\vec{\boldsymbol{x}}) - |B(0,5\lambda)|\chi_T(\vec{\boldsymbol{x}}),$$

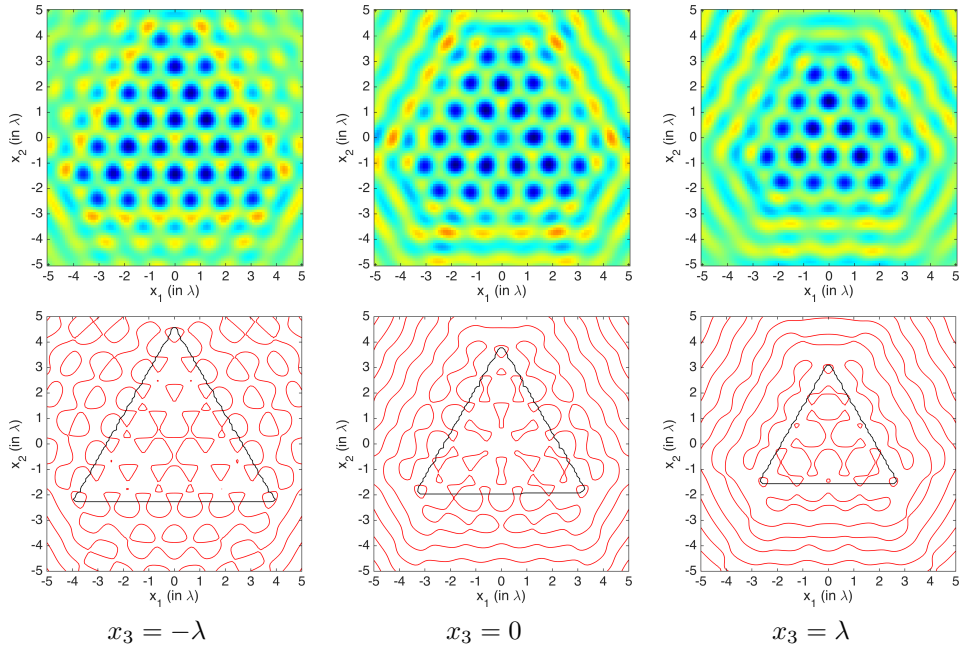



FIG. 1. *Approximation of a function $f$ with tetrahedral zero level set. The top row shows three $x_3$ constant slices of the real part of the approximation of $f$. The bottom row shows zero level sets of the original function $f$ (black) and the real part of the approximation (red) for each slice. The color scale in the top row ranges from -0.01 (blue) to 0.01 (red).*

where $|A|$ denotes the volume of some region $A$. We chose this $f$ because its nodal set is $\partial T$, the boundary of the tetrahedron, and because $\int f(\vec{\boldsymbol{x}})d\vec{\boldsymbol{x}} = 0$. This last property ensures that $\widehat{f}(\vec{\mathbf{0}}) = 0$, as is the case for all Herglotz wave functions. The function $f$ is sampled on a uniform grid with $256^3$ points in the cube $[-5\lambda, 5\lambda]^3$. This corresponds to a uniform grid in spatial frequency within the cube $[-12.8k, 12.8k]^3$ with identical number of points. The triangulation of $S(0,k)$ that we used consisted of 7292 triangles and was obtained using the DistMesh package [13]. The visualization of the resulting Herglotz wave function $u$ is done in slices $(x,y) \in [-5\lambda, 5\lambda]^2$ that are sampled with $100^2$ uniformly spaced points.

Since the asymptotic in Theorem 5 is not a projection, the resulting Herglotz wave function will be off by a scaling factor, which is why we include a comparison of the zero level sets in Figure 1. This numerical experiment illustrates the poor approximation that was expected in a volume. Indeed this function has significant Fourier components outside of $S(0,k)$ that are filtered out in $u$. Intuitively, we are trying to control a volume with only a two dimensional field (the Herglotz wave function density).

**4.2. Approximation on a plane.** We compare two methods for approximating a compactly supported bounded function $f$ by Helmholtz equation solutions: time reversal, and projection onto the space of Herglotz wave functions supported on the upper half of the sphere $S(0,k)$ and restricted to the plane $x_3 = 0$. As we saw in Theorem 7, the projection method is optimal and should give better approximations. This is confirmed in the numerical results we present here.

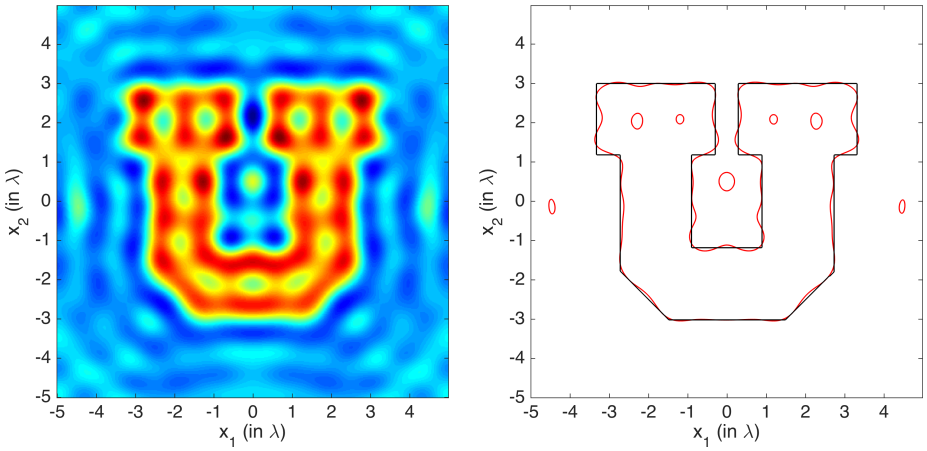



FIG. 2. *Approximating a function $f$ with "U" zero level set using time reversal. (a) shows the convolution of $f$ with $j_0(k|\cdot|)$. (b) shows zero level sets of $f$ (black) and of the convolution (red).*

**4.2.1. Time reversal approximation.** As explained in section 2.2, we can view time reversal as a convolution with kernel $(4\pi)^{-1}j_0(k|\cdot|)$, which is the tightest an entire solution to the Helmholtz equation can get. The function $f$ that we use is obtained from the University of Utah "U" logo by rescaling it so that it is about $6\lambda \times 6\lambda$, and setting $f(x) = 1$ inside the "U" and $f(x) = -1$ outside. We use a uniform grid on the square $[-5\lambda, 5\lambda]^2$ with $512^2$ points.

The time reversal approximation is shown in Figure 2. Theorem 9 shows that the time reversal procedure is equivalent, up a to a scaling factor, to filtering the function we wish to approximate with a filter response function that is supported in $B(0,k)$ but that boosts the frequencies with $|\boldsymbol{\xi}|$ close to $k$. We report only results up to a proportionality constant, and evaluate the performance of this method by comparing zero level sets. This procedure gives a Herglotz wave function approximation to $f$ that is suboptimal (see section 3.4) compared to the projection method we see next.

**4.2.2. Best approximation with Herglotz wave functions.** Following section 3, the best approximation by Herglotz wave functions of some function $f$ can be obtained by first filtering the function $f$, eliminating all spatial frequencies $\boldsymbol{\xi}$ with $|\boldsymbol{\xi}| > k$ and then using Lemma 6 to relate the filtered $f$ to a Herglotz density on $S(0,k)$.

To filter the function $f$ (i.e. projecting it onto $B_k$) we proceed as follows.

Step 1. Use a uniform spatial grid in a square to discretize $f$. By using the DFT, this gives an approximation to $\widehat{f}$ on a uniform (spatial) frequency grid.

Step 2. Restrict the $\widehat{f}$ computed in Step 1 to the ball $B(0,k)$.

Step 3. Calculate the inverse Fourier transform of $\widehat{f}|_{B(0,k)}$ (using the DFT).

The effect of filtering is shown in Figure 3, for the same function $f$ with University of Utah logo. As in the time reversal experiments we discretized $f$ on a uniform grid of the square $[-5\lambda, 5\lambda]^2$ with $512^2$ points. This corresponds to a spatial frequency grid on the square $[-25.6k, 25.6k]^2$ with the same number of points. Since the frequencies $|\boldsymbol{\xi}| > k$ have been eliminated, the corners in the zero level set of $f$ are smoothed out in the filtered version.

We recall that Lemma 6 gives a one-to-one relationship between functions in $B_k$

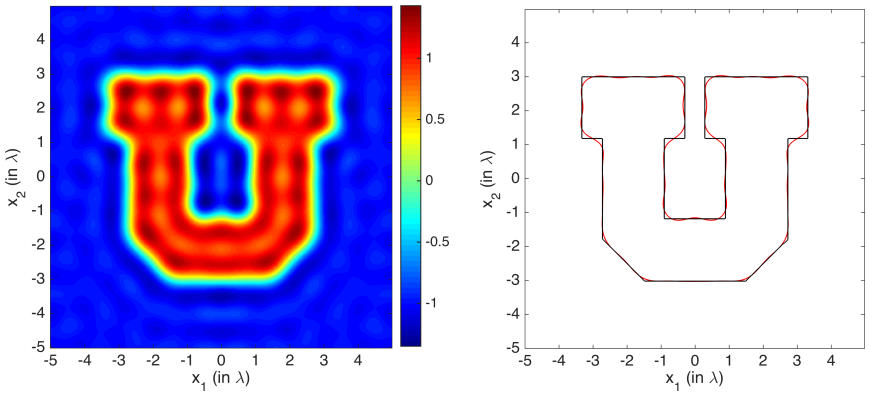



FIG. 3. *Approximating a function with "U" zero level set using the projection approach described in section 4.2. (a) Real part of projection of $f$ onto $S_{k+}|_{x_3=0}$. (b) Zero level set of real part of projection.*

and functions in $S_{k+}|_{x_3=0}$. In other words, the best approximation of $f$, which we obtained by projecting $f$ onto the space of band-limited functions $B_k$, corresponds to the restriction of a Herglotz wave function on the upper half of the sphere $S(0,k)$ to the plane $x_3 = 0$. The Herglotz density we used in the numerical experiment appears in Figure 4, where we can clearly see it is supported on the upper half sphere. We use this relation to evaluate a Herglotz wave function with density (16) on the plane $x_3 = 0$. This is done as follows.

Step 1. Discretize the sphere $S(0,k)$ with a Delaunay triangulation.

Step 2. Use a uniform spatial grid to discretize $f$. With the DFT these give an approximation of $\widehat{f}$ on a uniform (spatial) frequency grid.

Step 3. Interpolate $\widehat{f}$ on a uniform grid in the $x_3 = 0$ plane.

Step 4. The Herglotz wave function $u$ with density (16) is given by the integral (1) with $g$ given by (16), that we approximate by assuming it is piecewise constant on the triangles of the triangulation of $S(0,k)$.

For the particular numerical experiment we present, the triangulation of $S(0,k)$ consisted of 7292 triangles and was obtained using the DistMesh package [13]. The function $f$ was sampled on a uniform grid with $512^2$ points on the square $[-5\lambda, 5\lambda]^2$, which corresponds to a uniform grid in spatial frequency in the square $[-25.6k, 25.6k]^2$ with an identical number of points. As illustrated in Figure 5, the Herglotz wave function restricted to the $x_3 = 0$ plane is very close to the projection of $f$ onto $B_k$. Any differences are due to discretization errors, as they should be identical by Lemma 6. To emphasize that the approximation is a wave field, we also display in Figure 5 the field at the planes $x_3 = \pm\lambda$. As expected, the approximation degrades as we move away from the plane $x_3 = 0$. The $x_3 = \pm\lambda$ slices look identical because the Fourier transform of the function we considered has a relatively small imaginary part. Nevertheless the relative difference between the fields at $x_3 = \lambda$ and $x_3 = -\lambda$ is about 65%, when both real and imaginary parts are kept.

**5. Summary and future work.** We have shown that the problem of approximating a function by 3D Herglotz wave functions is not well-posed if we measure the misfit in a ball, but becomes well-posed if the misfit is measured in a plane. The solution to the approximation problem on a ball is asymptotically close to a time

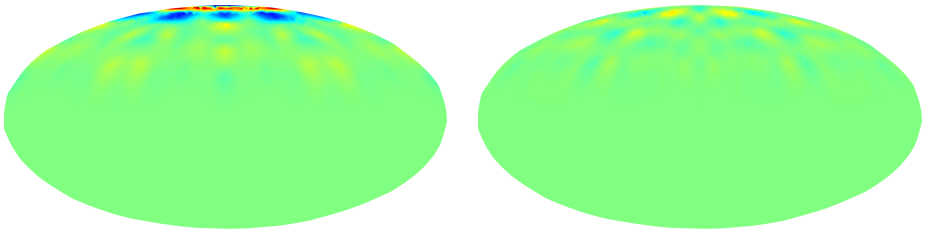


FIG. 4. *Real (left) and imaginary (right) parts of the Mollweide projection for the Herglotz wave function density used to obtain the approximation in Figure 5. The color scale ranges from -20 (blue) to 20 (red).*

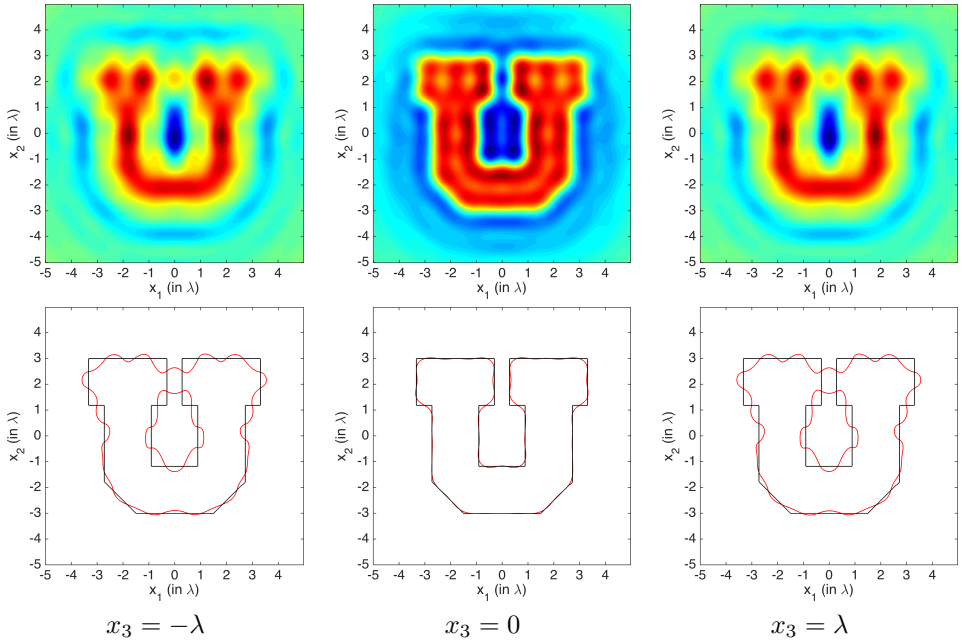



FIG. 5. *Best approximation of $f$ in $S_{k+}|_{x_3=0}$. The top row shows three slices of the real part of the approximation of $f$. The bottom row shows zero level sets of the original function $f$ (black) and the real part of the approximation (red). The color scale in the top row ranges from -2 (blue) to 1.5 (red).*

reversal experiment where the function to be approximated is regarded as a source density. The approximation problem in a plane is shown to be related to filtering the spatial frequencies of the function we wish to approximate. Our theoretical results are illustrated by numerical experiments showing that the approximation problem on a plane gives Helmholtz equation solutions with nodal set close to that of the function we approximate. We are currently studying other ways of measuring misfit to be able to design solutions to the Helmholtz equation with e.g., maxima along a given curve. This could be used to manipulate particles in a fluid with acoustic waves, in situations where the particles cluster about the anti-nodes of a wave.

**Acknowledgements.** FGV would like to thank Bart Raeymaekers and John Greenhall for insightful conversations on this topic.

## REFERENCES


[1] N. Bleistein, J. K. Cohen, and J. W. Stockwell, Jr. *Mathematics of multidimensional seismic imaging, migration, and inversion*, volume 13 of *Interdisciplinary Applied Mathematics*. Springer-Verlag, New York, 2001. Geophysics and Planetary Sciences.

[2] D. Colton and R. Kress. *Inverse acoustic and electromagnetic scattering theory*, volume 93 of *Applied Mathematical Sciences*. Springer-Verlag, Berlin, second edition, 1998.

[3] *NIST Digital Library of Mathematical Functions*. http://dlmf.nist.gov/, Release 1.0.15 of 2017-06-01. F. W. J. Olver, A. B. Olde Daalhuis, D. W. Lozier, B. I. Schneider, R. F. Boisvert, C. W. Clark, B. R. Miller and B. V. Saunders, eds.

[4] M. Fink. Time reversed acoustics. *Physics Today*, 50:34, March 1997.

[5] J. Garnier and G. Papanicolaou. *Passive imaging with ambient noise*. Cambridge University Press, Cambridge, 2016.

[6] L. P. Gor'kov. On the forces acting on a small particle in an acoustical field in an ideal fluid. *Soviet Physics Doklady*, 6:773, March 1962.

[7] J. Greenhall, F. Guevara Vasquez, and B. Raeymaekers. Continuous and unconstrained manipulation of micro-particles using phase-control of bulk acoustic waves. *Applied Physics Letters*, 103(7), 2013.

[8] J. Greenhall, F. Guevara Vasquez, and B. Raeymaekers. Ultrasound directed self-assembly of user-specified patterns of nanoparticles dispersed in a fluid medium. *Applied Physics Letters*, 108(10), 2016.

[9] F. Guevara Vasquez, G. W. Milton, and D. Onofrei. Exterior cloaking with active sources in two dimensional acoustics. *Wave Motion*, 48(6):515–524, 2011. Special Issue on Cloaking of Wave Motion.

[10] L. V. King. On the acoustic radiation pressure on spheres. *Proceedings of the Royal Society of London A: Mathematical, Physical and Engineering Sciences*, 147(861):212–240, 1934.

[11] D. A. B. Miller. On perfect cloaking. *Opt. Express*, 14(25):12457–12466, 2006.

[12] D. Onofrei. Active manipulation of fields modeled by the Helmholtz equation. *J. Integral Equations Appl.*, 26(4):553–579, 2014.

[13] P.-O. Persson and G. Strang. A simple mesh generator in Matlab. *SIAM Rev.*, 46(2):329–345, 2004.

[14] M. Prisbrey, J. Greenhall, F. Guevara Vasquez, and B. Raeymaekers. Ultrasound directed self-assembly of three-dimensional user-specified patterns of particles in a fluid medium. *Journal of Applied Physics*, 121, 2017.

[15] M. Settnes and H. Bruus. Forces acting on a small particle in an acoustical field in a viscous fluid. *Phys. Rev. E*, 85:016327, Jan 2012.

[16] D. Slepian. Prolate spheroidal wave functions, Fourier analysis and uncertainity. IV. Extensions to many dimensions; generalized prolate spheroidal functions. *Bell System Tech. J.*, 43:3009–3057, 1964.

[17] N. Weck. Approximation by Herglotz wave functions. *Math. Methods Appl. Sci.*, 27(2):155–162, 2004.

[18] K. Yosioka and Y. Kawasima. Acoustic radiation pressure on a compressible sphere. *Acta Acustica united with Acustica*, 5(3):167–173, 1955.